

Chapter 3 Experiments

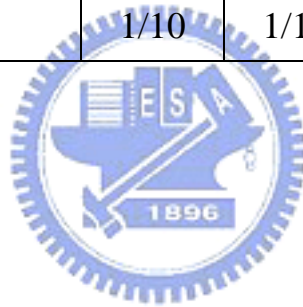
3-1 Sample preparations

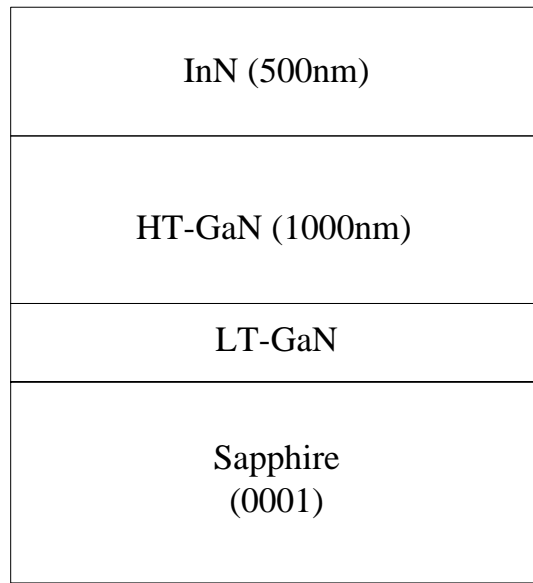
Wurtzite-InN samples were grown on GaN buffer layers upon sapphire (0001) substrates by pulsed-mode metal organic vapor phase epitaxy (MOVPE) using trimethylgallium (TMGa), trimethylindium (TMIn) and NH_3 as the sources. Sizes of InN dots were controlled by tuning deposition times of trimethylindium (TMIn) source from 10 sec to 20 sec or varying substrate temperatures (T_s) from 600 to 650 °C. The gas flow sequence basically consists of 6 cycles for the growth of InN dots. Each cycle has four steps: 20-sec TMIn (150 sccm) source step, 20-sec NH_3 (10000 sccm) source step and the intervened 10-sec NH_3 purge (18000 sccm) step in between. After growth of InN dots, the substrate temperature was decreased under a continuous flush of NH_3 gas for the growth of a 35 nm-thick GaN cap layer for optical measurements. Uncapping InN dots were used for the atomic force microscope (AFM) measurements. Table I summarizes the growth parameters of InN dots.

For reference, InN epilayers with layer thickness of 500 nm were also fabricated at T_s of 600°C to 650°C with TMIn of 360 sccm and NH_3 of 15000 sccm. The Hall measurement shows the best room-temperature mobility of the InN epilayer was about 1300 $\text{cm}^2/\text{V}\cdot\text{s}$. Background electron concentrations were 6.4×10^{18} , 7.9×10^{18} , and $1.3 \times 10^{19} \text{ cm}^{-3}$.

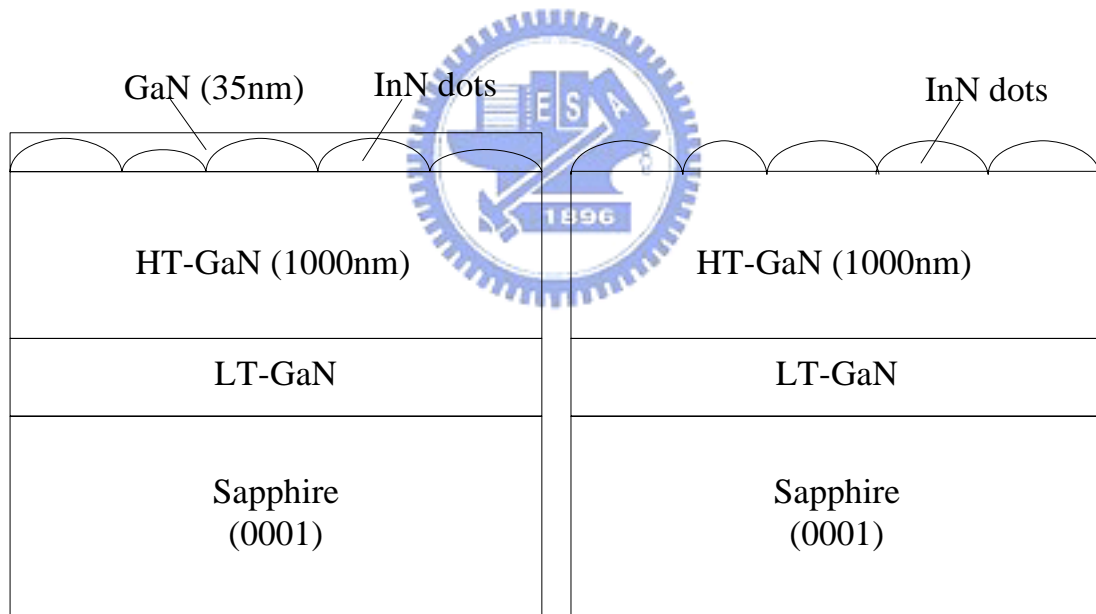
Table I. Growth parameters of InN dot samples.

Sample	A	B	C	D
Substrate temperature (°C)	600	625	650	625
TMIn deposition time (sec/cycle)	20	20	20	10
Average dot height(nm)/width (nm)	18/180	28/216	32/253	24/177
Aspect ratio	1/10	1/13	1/13	1/14





(a)



(b)

(c)

Fig. 3-1. Sample structures: (a) InN epilayer, (b) embedded InN dots for optical measurements and (c) uncapped InN dots for the morphological measurement.

3-2 Atomic force microscopy (AFM) system

A NT-MDT SOLVER P47H AFM system was used to investigate the morphology of InN nano-dot samples by a scanning tip located at the free end of a cantilever attached to the scanner of the AFM system. The scanner made of the piezoelectric crystal controls the tip's movement along the X-Y plane and Z-direction. The piezoelectric crystal will expand or shrink proportion to the applied electric voltage. During scanning, a laser beam detects the cantilever's deflection from the initial position and sends the signal to the scanner's control system. When the tip is driven close to the sample surface, the atomic force between the tip and sample will affect the deflection of the cantilever, and reflective optical signals due to the tip displacement are analyzed to transform as the sample's morphology.

There are three traditional modes, the contact mode, the non-contact mode and the tapping mode, to investigate sample morphology. We used the tapping mode to measure the morphology and to avoid the destruction of the probe and samples instead of the contact mode or the non-contact mode. The morphology of InN dots measured by the tapping mode was used to obtain the size shape, dot densities and size distribution. The diagram of AFM system is shown in Fig. 3-2.

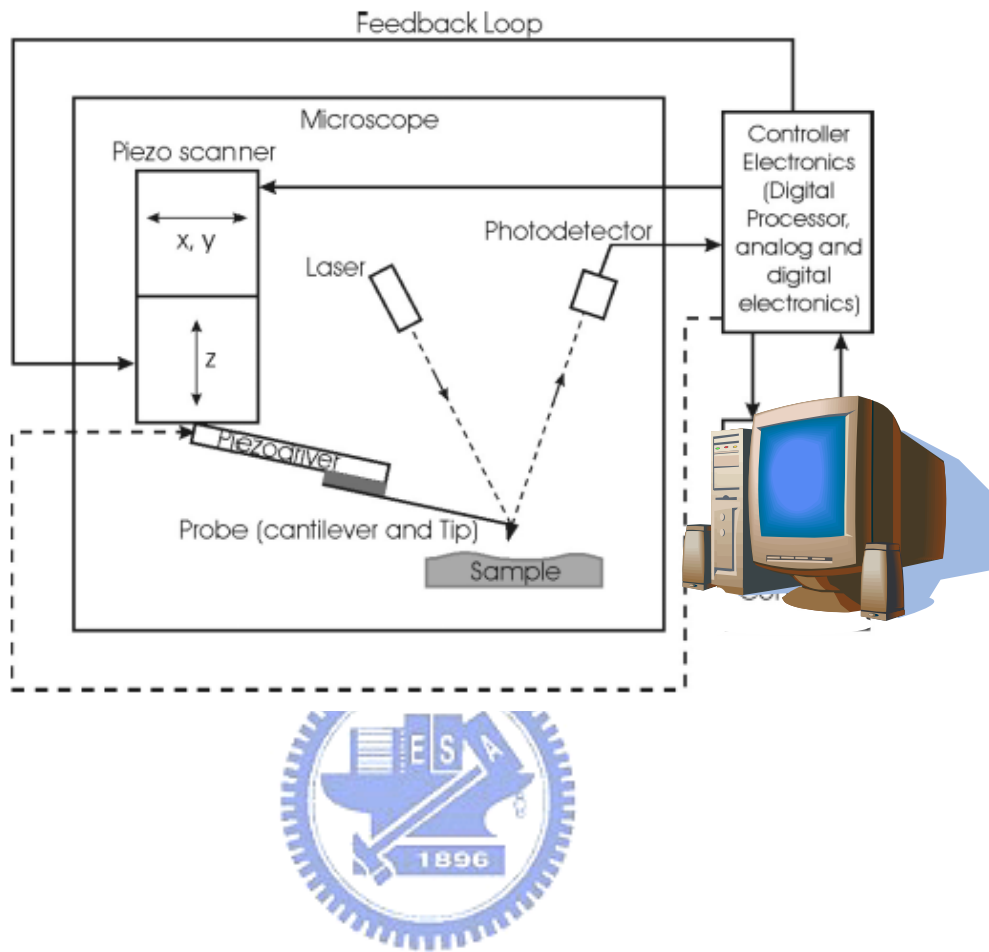


Fig. 3-2. Schematic diagram of an AFM system.

3-3 Photoluminescence (PL) system

As shown in Fig. 3-3, PL measurements were performed by using the 488-nm laser line of an argon-ion laser as the excitation source. The incident beam was chopped and focused by a lens ($f=10$ cm). The focused spot size was about 1 mm^2 . PL emission was collected by another lens ($f=15$ cm) and focused by the third lens ($f=28$ cm) to the entrance slit of a mono-chromator (Spex 270M). The signals were detected by an uncooled extended InGaAs photo-detector (cut-off wavelength at $2.05\text{ }\mu\text{m}$) and amplified by the standard lock-in amplifier technique. Output of the lock-in amplifier was analyzed by the Spectra ACQ2.

For temperature-dependent PL measurements, samples were mounted on a cold finger of a closed-cycle refrigerator system. The temperature was varied from 13 K to 300 K.



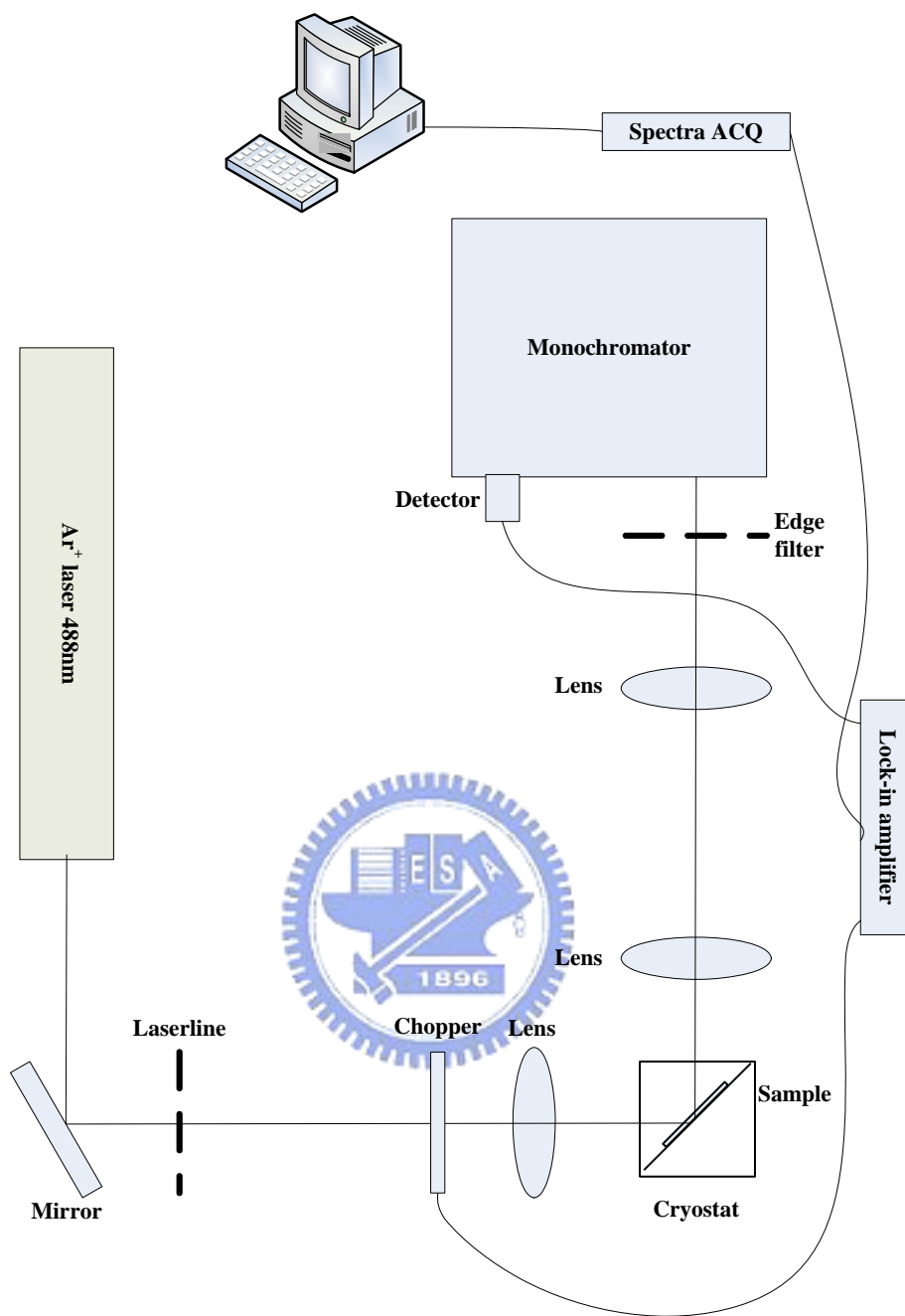


Fig. 3-3. Schematic diagram of the PL system.